Electrochemical preparation of Pd nanorods with high-index facets†

Na Tian, Zhi-You Zhou and Shi-Gang Sun*

Received (in Cambridge, UK) 5th November 2008, Accepted 15th December 2008
First published as an Advance Article on the web 22nd January 2009
DOI: 10.1039/b819751b

Fivefold twinned Pd nanorods bounded by high-index facets of {*hk*0} or {*hkk*} were prepared by an electrochemical method and tested as electrocatalysts of high activity for ethanol oxidation.

Pd nanostructures are of great interest due to their extensive applications in gas sensor[1] and diverse catalytic fields, such as electrooxidation of formic acid and ethanol,[2] automotive exhaust purification,[3] and Suzuki coupling reactions.[4] It is known that the catalytic activity of metal nanoparticles highly depends on their shape or surface atomic arrangement;[5] therefore, shape-controlled synthesis of Pd nanocrystals has attracted intensive interest.[6] Xia and co-workers have synthesized a series of Pd nanocrystals with different shapes, such as cube, octahedron, decahedron, icosahedron, nanorod and nanobar.[7] All these Pd nanocrystals are bounded by low-index facets, *i.e.*, {111}, {100} or {110} facets. High-index facets with atomic steps and kinks are more desirable in catalysis, since they usually exhibit much higher activity than low-index facets.[8] Unfortunately, it is very challenging to synthesize metal nanocrystals enclosed by high-index facets due to their high surface energy. We have developed recently an electrochemically shape-controlled synthesis method by using a square-wave potential, and prepared Pt, Pd tetrahexahedral nanocrystals and Pt nanorods with {*hk*0} high-index facets.[9] In this communication, we demonstrate further that fivefold twinned Pd nanorods with high-index facets of {*hkk*} or {*hk*0} ($h > k$) can be prepared by using the method with well-controlled conditions. It has proved that the Pd nanorods exhibit high catalytic activity towards electrooxidation of ethanol due to the high-index facets.

Electrochemical preparation was carried out in a standard three-electrode cell connected to a PAR 263A potentiostat (EG&G), with a platinum foil counter electrode and a saturated calomel electrode (SCE) at room temperature. All electrode potentials were quoted *versus* the SCE scale. The working electrode was a glassy carbon disk (GC, ϕ = 6 mm). Pd nanorods were electrodeposited on the GC substrate in 5 mM $PdCl_2$ + 0.1 M $HClO_4$ solution by using the method of square-wave potential at 100 Hz for 20 min. By changing the lower (E_L) and upper (E_U) potential limits, Pd nanorods with different shapes were obtained. The structure of the nanorods was characterized by scanning electron microscopy (SEM, LEO1530) and transmission electron microscopy (TEM, FEI Tecnai-F30).

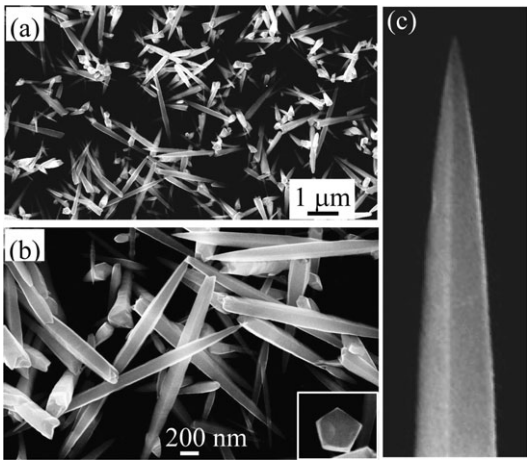

Fig. 1 (a) Low and (b) high magnification SEM images of Pd nanorods (type-I) prepared at E_L = −0.15 V, E_U = 0.65 V; the inset to (b) shows the pentagonal projection of a Pd nanorod. (c) SEM image of a tip of a Pd nanorod.

Fig. 1a shows a SEM image of Pd nanorods (type-I) prepared at E_L = −0.15 V and E_U = 0.65 V. The nanorods are not uniform in diameter along the longitudinal axis. The average diameter measured at the middle part is about 190 nm, and the average length is about 2.0 μm. The distribution density of the Pd nanorods is about 2.5 × 10^8 cm^{-2}. Fig. 1b illustrates a high-magnification SEM image of Pd nanorods, from which we can see that the nanorods are highly faceted. The projection of the Pd nanorod is a pentagon (see the inset to Fig. 1b), which indicates that it has a pentagonal cross-section. At the end of the Pd nanorods, two or three facets can be discerned. The SEM image in Fig. 1c illustrates a Pd nanorod tip, which is a pentagonal pyramidal shape on the basis of the cross-section. It is worthwhile to note that, although most of the nanorods (~70%) have a broken end, they still preserve smooth facets, *i.e.*, their surfaces are similar to those of Pd nanorods with two tips.

The shape of the Pd nanorods can be tuned by changing the potential limit of the square wave. Fig. 2a depicts a SEM image of Pd nanorods (type-II) obtained with E_L = 0.15 V and E_U = 0.85 V. The distribution density of the Pd nanorods was decreased considerably to 1.5 × 10^7 cm^{-2} due to the growth at higher potential. Besides, many irregular faceted Pd nanoparticles (~100 nm) grew on the GC substrate. The yield of type-II Pd nanorods was estimated to be about 50% based on Pd volume. The Pd nanorods are not uniform in size due to progressive nucleation during the growth, and their length

State Key Laboratory of Physical Chemistry of Solid Surfaces, Department of Chemistry, College of Chemistry and Chemical Engineering, Xiamen University, Xiamen 361005, China. E-mail: sgsun@xmu.edu.cn
† Electronic supplementary information (ESI) available: Shapes of the ends and Miller indices of the nanorods; voltammograms. See DOI: 10.1039/b819751b

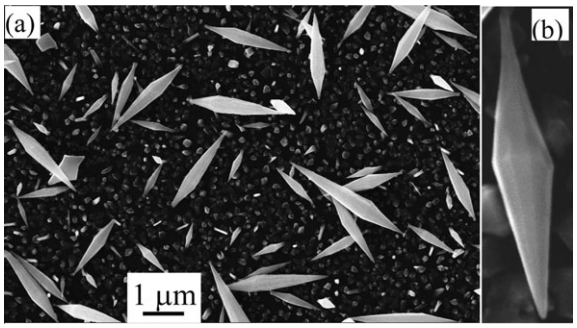

Fig. 2 (a) SEM image of Pd nanorods (type-II) prepared at E_L = 0.15 V, E_U = 0.85 V. (b) High magnification SEM image of a Pd nanorod, showing the decagonal bipyramidal shape.

varies from 0.5 to 3 μm. A magnified SEM image of a Pd nanorod is shown in Fig. 2b. Five facets can be observed clearly at each end, indicating that the tip is enclosed by ten facets. Therefore, the shape of the type-II nanorod is a decagonal bipyramid, which is significantly different from the pentagonal pyramid of the type-I Pd nanorod (Fig. 1c).

The crystal structure of the Pd nanorods was analyzed by selected-area electron diffraction (SAED). Both type-I and type-II Pd nanorods can provide two typical SAED patterns, as shown in Fig. 3a and b. Each diffraction pattern contains two sets of diffraction from the face-centered cubic Pd. In Fig. 3a, the square (solid line) and rectangular (dashed line) symmetrical diffractions correspond to [001] and [$\bar{1}$12] zone axes, respectively. The diffraction pattern in Fig. 3b was obtained after rotating the nanorod by 18° along the longitudinal axis. Two diffractions corresponding to [1$\bar{1}$0] (solid line) and [1$\bar{1}\bar{1}$] (dashed line) zone axes can be observed. A few additional weak diffraction spots (*e.g.*, marked by arrows in Fig. 3a) originate from double diffractions.[10] These SAED characters are in good agreement with those obtained from fivefold twinned metal nanorods reported previously,[11] demonstrating that the as-prepared Pd nanorods are of a fivefold twinned structure.

The shape of a conventional fivefold twinned nanorod is a pentagonal prism with {100} facets, capped by two pentagonal pyramids with {111} facets,[11] as illustrated in Fig. 4a. Clearly, this shape is quite different from that of the type-I or type-II Pd nanorods. We found that if the {111} facets of a nanorod tip (Fig. 4b) are changed into {*hkk*} ($h > k > 0$) high-index facets, although the tip keeps the shape of a pentagonal pyramid,[12] the taper of the nanorod tip becomes steeper, as illustrated in Fig. 4c; if the {111} facets are changed into {*hk*0}

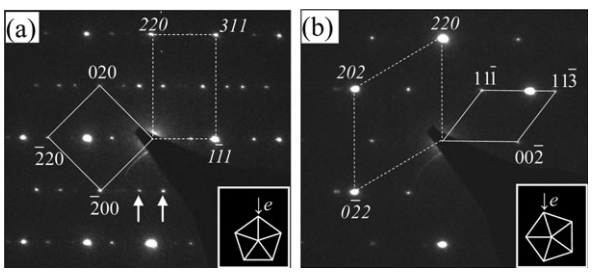

Fig. 3 (a), (b) Two typical patterns of selected-area electron diffraction (SAED) obtained from both type-I and type-II Pd nanorods, demonstrating that the nanorods are of a fivefold twinned structure.

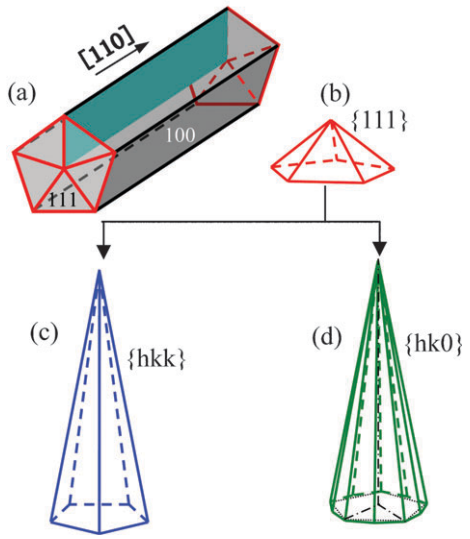

Fig. 4 (a) Model of a conventional fivefold twinned nanorod; (b), (c), and (d) tips of nanorods bounded by {111}, {*hkk*} and {*hk*0} ($h > k$) facets, respectively.

($h > k > 0$) high-index facets, the tip will change from a pentagonal pyramid into a decagonal pyramid (Fig. 4d). Fig. S1 and S2 in the ESI† give the detailed illustrations for the transformation. Obviously, the elongated pentagonal pyramid shown in Fig. 4c is very similar to the tip of type-I Pd nanorods, and the decagonal pyramid is similar to the tip of type-II Pd nanorods. By measuring the geometric parameters of the tip of the Pd nanorods, *e.g.*, the ratio of height to base width, we can determine that the surfaces of type-I Pd nanorods range from {10, 1, 1} to {15, 1, 1} facets, and the surfaces of type-II Pd nanorods vary from {310} to {610} facets (see ESI†, Fig. S3).

Similar to the growth mechanism of tetrahexahedral Pt nanocrystals enclosed by {*hk*0} facets,[9] the formation of {*hkk*} and {*hk*0} high-index facets on Pd nanorods can also be related to dynamic oxygen adsorption/desorption on the Pd surface, leading to that only open-structure surfaces with low coordinated atoms can survive. The onset potential of the formation of Pd surface oxide in 0.1 M $HClO_4$ is about 0.34 V according to the cyclic voltammogram of Pd nanorods (see ESI†, Fig. S4). The oxidation degree of Pd surfaces will increase with increasing E_U. The difference in surface structure on the type-II and type-I Pd nanorods indicates that the more intensive surface reconstruction by oxygen adsorption/desorption (E_U: 0.85 V *vs.* 0.65 V) will favor the formation of surfaces with lower coordinated atoms (coordination numbers: 6 and 7 for {*hk*0} and {*hkk*} facets, respectively). Besides, the broken end observed on the type-I Pd nanorods may be caused by crystal defects (see discussion in ESI†).

Electrocatalytic oxidation of ethanol in alkaline solution was used as a test reaction to characterize the catalytic activity of Pd nanorods. Fig. 5a compares cyclic voltammograms of the type-I Pd nanorods (solid line) and a commercial Pd black catalyst (Johnson Matthey, dashed line) in 0.1 M NaOH + 0.1 M ethanol solution. The oxidation current has been normalized to the electroactive surface area of Pd, which was measured from the electric charge of reduction of

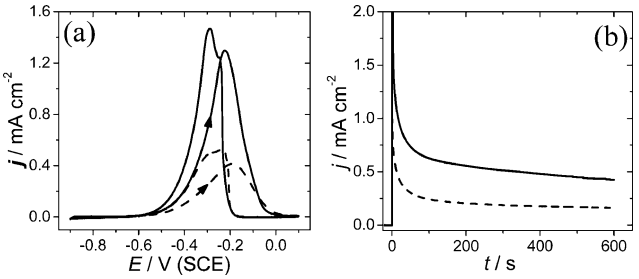

Fig. 5 (a) Cyclic voltammograms (10 mV s^{-1}) and (b) current–time curves, measured at −0.30 V, of ethanol oxidation on type-I Pd nanorods (solid line) and commercial Pd black catalyst (dashed line) in 0.1 M ethanol + 0.1 M NaOH solution.

monolayer Pd oxide with an assumption of 424 μC cm^{-2}, according to the method proposed by Woods[13] (see ESI†, Fig. S5). The catalytic activity of the Pd nanorods is superior to that of the Pd black catalyst. The peak current densities of ethanol oxidation on the Pd nanorods in the positive- and negative-going potential scans are 1.30 and 1.47 mA cm^{-2}, respectively. Corresponding current densities obtained on the Pd black catalyst are only 0.41 and 0.53 mA cm^{-2}. Fig. 5b shows the current–time curves of ethanol oxidation at −0.30 V. The oxidation current density on the Pd nanorods is double of that measured on the Pd black. The 2–3 fold enhancement in activity may be correlated with the {*hkk*} high-index facets on the Pd nanorods. We also tested the catalytic activity of the sample of type-II Pd nanorods shown in Fig. 2, which is also higher than that of the Pd black catalyst (see ESI†, Fig. S6). However, the intrinsic catalytic activity of the type-II Pd nanorods cannot be precisely evaluated, since the distribution density of the nanorods is relatively low and the contribution of irregular faceted nanoparticles cannot be ignored.

In summary, fivefold twinned Pd nanorods with {*hkk*} or {*hk*0} high-index facets were prepared by an electrochemical square-wave potential method with well-controlled potential limits. The formation of different facets is attributed to the different degrees of surface reconstruction induced by oxygen adsorption/desorption. This result indicates that changing the potential limits of a square-wave potential is a convenient method to tune the surface structure of Pd nanocrystals. Systematic studies of the effect of square-wave potential on the shape of Pd nanocrystals and the preparation of Pd nanorods with smaller sizes for practical application are in progress in our laboratory. The Pd nanorods with {*hkk*} high-index facets exhibit 2–3 times higher catalytic activity per unit surface area than commercial Pd black catalyst towards the electrooxidation of ethanol in alkaline solution. The study is of significance for shape-controlled synthesis of metal nanorods, as well as in the preparation of catalysts of open surface structure with high activity for electrocatalysis and electrochemical sensors.

This work was supported by the Natural Science Foundation of China (Grant Nos. 20873113, 20833005, 20828005, and 20673091), the Ministry of Science and Technology of China (Grant Nos. 2009CB220102 and 2007DFA40890), the Research Fund for New Teachers of the Doctoral Program of Higher Education of China (Grant No. 200803841035) and the Fujian Provincial Department of Science and Technology (Grant Nos. 2008F3099 and 2008I0025). We thank Prof. Z. L. Wang and Dr Y. Ding from the Georgia Institute of Technology for their helpful discussions on the structure of Pd nanorods.

Notes and references

1 F. Favier, E. C. Walter, M. P. Zach, T. Benter and R. M. Penner, *Science*, 2001, **293**, 2227.
2 W. P. Zhou, A. Lewera, R. Larsen, R. I. Masel, P. S. Bagus and A. Wieckowski, *J. Phys. Chem. B*, 2006, **110**, 13393; C. W. Xu, H. Wang, P. K. Shen and S. P. Jiang, *Adv. Mater.*, 2007, **19**, 4256.
3 H. S. Gandhi, G. W. Graham and R. W. McCabe, *J. Catal.*, 2003, **216**, 433.
4 R. Narayanan and M. A. El-Sayed, *J. Am. Chem. Soc.*, 2003, **125**, 8340.
5 F. J. Vidal-Iglesias, J. Solla-Gullon, P. Rodriguez, E. Herrero, V. Montiel, J. M. Feliu and A. Aldaz, *Electrochem. Commun.*, 2004, **6**, 1080; K. M. Bratlie, H. Lee, K. Komvopoulos, P. D. Yang and G. A. Somorjai, *Nano Lett.*, 2007, **7**, 3097; C. Wang, H. Daimon, T. Onodera, T. Koda and S. H. Sun, *Angew. Chem., Int. Ed.*, 2008, **47**, 3588.
6 A. R. Tao, S. Habas and P. D. Yang, *Small*, 2008, **4**, 310; S. E. Habas, H. Lee, V. Radmilovic, G. A. Somorjai and P. Yang, *Nat. Mater.*, 2007, **6**, 692; F. R. Fan, D. Y. Liu, Y. F. Wu, S. Duan, Z. X. Xie, Z. Y. Jiang and Z. Q. Tian, *J. Am. Chem. Soc.*, 2008, **130**, 6949; H. Meng, S. Sun, J. P. Masse and J. P. Dodelet, *Chem. Mater.*, 2008, **20**, 6998; Y. J. Xiong and Y. N. Xia, *Adv. Mater.*, 2007, **19**, 3385.
7 B. Lim, Y. J. Xiong and Y. N. Xia, *Angew. Chem., Int. Ed.*, 2007, **46**, 9279; Y. J. Xiong, H. G. Cai, B. J. Wiley, J. G. Wang, M. J. Kim and Y. N. Xia, *J. Am. Chem. Soc.*, 2007, **129**, 3665; Y. J. Xiong, H. G. Cai, Y. D. Yin and Y. N. Xia, *Chem. Phys. Lett.*, 2007, **440**, 273; Y. J. Xiong, J. M. McLellan, Y. D. Yin and Y. N. Xia, *Angew. Chem., Int. Ed.*, 2007, **46**, 790; Y. J. Xiong, J. M. McLellan, J. Y. Chen, Y. D. Yin, Z. Y. Li and Y. N. Xia, *J. Am. Chem. Soc.*, 2005, **127**, 17118.
8 G. A. Somorjai, *Chemistry in Two Dimensions: Surfaces*, Cornell University Press, Ithaca, 1981.
9 N. Tian, Z. Y. Zhou, S. G. Sun, Y. Ding and Z. L. Wang, *Science*, 2007, **316**, 732; Z. Y. Zhou, N. Tian, Z. Z. Huang, D. J. Chen and S. G. Sun, *Faraday Discuss.*, 2008, **140**, 81; N. Tian, Z. Y. Zhou and S. G. Sun, *J. Phys. Chem. C*, 2008, **112**, 19801.
10 H. Hofmeister, S. A. Nepijko, D. N. Ievlev, W. Schulze and G. Ertl, *J. Cryst. Growth*, 2002, **234**, 773.
11 I. Lisiecki, A. Filankembo, H. Sack-Kongehl, K. Weiss, M. P. Pileni and J. Urban, *Phys. Rev. B: Condens. Matter Mater. Phys.*, 2000, **61**, 4968; C. Lofton and W. Sigmund, *Adv. Funct. Mater.*, 2005, **15**, 1197; Y. G. Sun, B. Mayers, T. Herricks and Y. N. Xia, *Nano Lett.*, 2003, **3**, 955; T. Ling, H. M. Yu, X. H. Liu, Z. Y. Shen and J. Zhu, *Cryst. Growth Des.*, 2008, **8**, 4340.
12 M. Z. Liu and P. Guyot-Sionnest, *J. Phys. Chem. B*, 2005, **109**, 22192.
13 D. A. J. Rand and R. Woods, *J. Electroanal. Chem.*, 1971, **31**, 29.

